Renal Cortical Scarring: ^{68}Ga-PSMA-11 PET Versus ^{99m}Tc-DMSA Scanning in a Case of Pyelonephritis

Ismet Sarikaya[1], Ahmed Alqallaf[2], Ali Sarikaya[3], Ali Baqer[4], and Nafisa Kazem[5]

[1]Department of Nuclear Medicine, Mubarak Al-Kabeer Hospital, Kuwait University, Kuwait City, Kuwait; [2]Department of Nephrology, Mubarak Al-Kabeer Hospital, Kuwait University, Kuwait City, Kuwait; [3]Department of Nuclear Medicine, Trakya University, Edirne, Turkey; [4]Department of Nuclear Medicine, Mubarak Al-Kabeer Hospital, Kuwait University, Kuwait City, Kuwait; and [5]Department of Nuclear Medicine, Mubarak Al-Kabeer Hospital, Kuwait University, Kuwait City, Kuwait

We previously reported the ^{68}Ga-labeled prostate-specific membrane antigen (PSMA)-11 and ^{99m}Tc-dimercaptosuccinic acid (DMSA) images of the first patient in our prospective research comparing renal ^{68}Ga-PSMA-11 PET with ^{99m}Tc-DMSA scanning in adults with pyelonephritis. Here, we present the renal cortical ^{68}Ga-PSMA-11 PET and ^{99m}Tc-DMSA images of our second patient, who had chronic recurring pyelonephritis and demonstrated renal parenchymal defects secondary to scarring in the kidney.

Key Words: DMSA scan; ^{68}Ga-PSMA-11; PET; pyelonephritis; renal scar

J Nucl Med Technol 2022; 50:49–53
DOI: 10.2967/jnmt.121.262415

Renal cortical imaging with ^{99m}Tc-dimercaptosuccinic acid (DMSA) is widely used to detect renal parenchymal changes due to acute pyelonephritis (reduced uptake) and renal sequelae (scars) (absence of uptake) 6 mo after acute infection (*1*). ^{99m}Tc-DMSA scanning is also used to quantify differential renal function, detect various renal abnormalities, and assess the functional status of multicystic kidneys (*1*). The ability to depict renal scarring via a ^{99m}Tc-DMSA scanning is important because scarring is a common cause of hypertension and because extensive scarring can lead to progressive renal impairment and end-stage renal disease (*2*). The presence of scarring can lead to a change in the treatment plan, such as starting different antibiotics, starting corticosteroids, treating bladder or bowel dysfunction, or performing surgical interventions to prevent further scar formation (*3*). Potential new treatments such as cyclooxygenase-2 inhibitors, superoxide dismutases, and matrix metalloproteinase-9 inhibitors may also prevent scar formation (*3*). A nonfunctioning or poorly functioning kidney due to chronic recurrent pyelonephritis may be surgically removed, as it may cause systemic complications such as sepsis, septic shock, and hypertension (*2*).

^{68}Ga-labeled prostate-specific membrane antigen (^{68}Ga-PSMA) ligands or inhibitors are currently used for initial staging of high-risk prostate cancer and, in cases of biochemical recurrence, for identifying the site of recurrence (*4–6*). These radiotracers also exhibit high physiologic uptake in the renal cortex. PSMA is a type II transmembrane protein, also known as glutamate carboxypeptidase II or folate hydrolase, which is found mainly in prostate tissue and is overexpressed in prostate cancer, in some extraprostatic normal tissues such as the kidneys and salivary glands, and in various other malignancies (*7–9*). Immunohistochemical analyses demonstrated detectable PSMA levels in the brush borders and apical cytoplasm of a subset of proximal renal tubules (*7*,*10*). The reason for the presence of PSMA in the renal proximal tubules is unknown but may be due to folate metabolism—that is, potential reuptake of folate in the kidneys (*11*).

We previously published ^{68}Ga-PSMA-11 PET images of the renal cortex of prostate cancer patients with and without cortical defects caused by various sizes of cysts (*2*,*12*,*13*). Given the high renal cortical uptake and excellent renal parenchymal distribution of ^{68}Ga-PSMA-11, we started a prospective research study comparing renal ^{68}Ga-PSMA-11 PET with ^{99m}Tc-DMSA scanning in adults with pyelonephritis. Our study was interrupted by the coronavirus disease 2020 Pandemic, but renal ^{68}Ga-PSMA-11 PET and ^{99m}Tc-DMSA images of our first patient have been published (*14*). In our first patient, neither ^{68}Ga-PSMA-11 PET nor ^{99m}Tc-DMSA scanning showed cortical defects, but ^{68}Ga-PSMA-11 PET demonstrated image quality superior to that of ^{99m}Tc-DMSA scanning. In the current report, we present renal ^{68}Ga-PSMA-11 PET and ^{99m}Tc-DMSA images of our second patient, who demonstrated cortical defects caused by scars.

MATERIALS AND METHODS

Our prospective study was approved by the Ethical Committee of the Health Sciences Center at Kuwait University and the Kuwait Ministry of Health. The study was conducted at Mubarak Al-Kabeer Hospital in Kuwait.

Received Apr. 8, 2021; revision accepted May 20, 2021.
For correspondence or reprints, contact Ismet Sarikaya (isarikaya99@yahoo.com).
Published online Jul. 30, 2021.

The patient provided written informed consent before the study. We obtained ^{68}Ga-PSMA-11 PET/CT and DMSA images of the kidneys.

^{68}Ga-PSMA ligand (PSMA-11) was radiolabeled at another institute (Radiopharmacy Unit at Kuwait Cancer Control Center) using a ^{68}Ge/^{68}Ga generator and a manual synthesis module (Isotope Technologies Garching).

Renal PET/CT images were obtained on a time-of-flight PET/CT camera (Philips Gemini) 60 min after intravenous injection of 48.1 MBq (1.3 mCi) of ^{68}Ga-PSMA-11. We intentionally used a low activity to reduce the radiation dose to the patient. A low-dose, unenhanced CT scan of the region of the kidneys was obtained for attenuation correction, anatomic localization, and gross anatomic correlation before the PET acquisition (30 mAs, 120 kV, pitch of 0.829, 0.5-s rotation time, 64 × 0.625 collimation, and 5-mm slice thickness). The PET acquisition time was 10 min per bed position for 2 bed positions. Because a low dose of activity was administered, the image acquisition time was longer than usual. The PET images were corrected for attenuation on the basis of the CT data, reconstructed using a standard iterative algorithm, and reformatted into transaxial, coronal, and sagittal slices. Maximum-intensity-projection images were also generated. Because of intense activity in the kidneys, the PET images were reviewed in a low-intensity setting to better assess the renal cortical uptake and distribution. Attenuation-corrected (AC) PET images, uncorrected (non-AC) PET images, PET/CT images, and low-dose CT images were reviewed to assess the anatomic location, size, and morphology of the kidneys; the uptake and distribution of radiotracer in the renal parenchyma; and any parenchymal defects or other abnormalities. Quantification of renal ^{68}Ga-PSMA-11 uptake was also performed. Because of unexpected high splenic uptake in this patient, we could not use automated volume-of-interest analysis with the software we had. We manually drew regions of interest around the kidneys in multiple transaxial slices to calculate the total activity in each kidney. In addition, we measured SUV_{max} and SUV_{mean} in both kidneys in both normal areas and areas with a parenchymal defect by placing a spheric region of interest over the renal cortex without exceeding the renal border.

Four days after PET imaging, ^{99m}Tc-DMSA images were obtained 3 h after intravenous injection of 111 MBq (3 mCi) of ^{99m}Tc-DMSA using a Symbia S SPECT scanner (Siemens) equipped with a high-resolution parallel-hole collimator. Multiple planar images were obtained in anterior, posterior, right posterior oblique, and left posterior oblique projections (10 min each, with a 20% window centered at 140 keV, a 256 × 256 matrix, and a zoom of 1.3). SPECT images of the kidneys were also obtained (a 20-s acquisition per view, 60 views, a 360° rotation, a 128 × 128 matrix, no zoom, and a 20% window centered at 140 keV). A standard iterative algorithm was used for image reconstruction. Images were reformatted into transaxial, coronal, and sagittal views. Uptake for each kidney was quantified using anterior and posterior planar images and the geometric mean.

RESULTS

The patient was a 49-y-old woman with a history of recurring pyelonephritis over the previous 14 mo. The last episode was a severe emphysematous pyelonephritis that occurred 2 mo before the current study (positive urine culture for *Candida albicans*) and was treated with antibiotics for 1 mo as an inpatient treatment. At the time of the study, the patient did not have any symptoms and urine cultures were negative. Renal ultrasound performed a month before the study demonstrated a dilated left renal pelvis and calyces with stones, preserved cortical thickness, and corticomedullary differentiation.

Planar and SPECT ^{99m}Tc-DMSA images demonstrated cortical defects, reduced uptake, and cortical irregularity in the upper and lower poles of the left kidney (Fig. 1). In the right kidney, no cortical defects were identified, with only slightly reduced uptake in the upper and lower poles, which could be a normal finding.

In the upper pole of the right kidney, the AC PET images had an artifact that seemed secondary to some possible unilateral patient motion that occurred as the patient passed urine during imaging. AC PET also showed reduced uptake and cortical defects in the upper and lower poles of the left kidney (Fig. 2). Splenic uptake was higher than usual in this patient, likely because of ^{68}Ga-colloid formation. In the normal physiologic distribution of ^{68}Ga-PSMA-11, splenic uptake is much lower than renal uptake and does not interfere with image interpretation (Fig. 3).

Non-AC PET images demonstrated similar findings to ^{99m}Tc-DMSA images, with cortical defects, reduced uptake, and irregularity in the upper and lower poles of the left kidney (Fig. 1). In the upper and lower poles of the right kidney, there was mildly reduced uptake similar to that on ^{99m}Tc-DMSA images. Bowel activity in the left upper quadrant did not affect the assessment of the left kidney but caused some overlap on the left kidney on maximum-intensity-projection images. Low-dose CT demonstrated small calculi in the lower pole of the left kidney. There were no cysts in the kidneys on low-dose CT.

Renal uptake was 35.5% on the left and 64.5% on the right with ^{99m}Tc-DMSA and 34.5% on the left and 65.5% on the right with ^{68}Ga-PSMA-11.

SUV_{max} and SUV_{mean} were 53 and 43, respectively, in the normal right-kidney parenchyma. In the left kidney, SUV_{max} and SUV_{mean} were 6.4 and 4, respectively, for the upper pole; 21.6 and 17.6, respectively, for the lower pole; and 52 and 41, respectively, for the mid cortical region.

DISCUSSION

^{99m}Tc-DMSA scanning is the current gold standard to assess the renal parenchyma and detect renal scarring, as has been described in detail in our recently published articles (*2*,*12*–*14*). Identification of renal scarring in patents with pyelonephritis is important because scarring is a common cause of hypertension and extensive scarring can cause progressive loss of renal function (*2*). In the management of patients with scarring due to pyelonephritis, further scarring might be prevented by a change in treatment plan, such as starting different antibiotics, supporting with other medications, treating bladder and bowel dysfunction, or performing surgical intervention (correcting vesicoureteral reflux) (*3*).

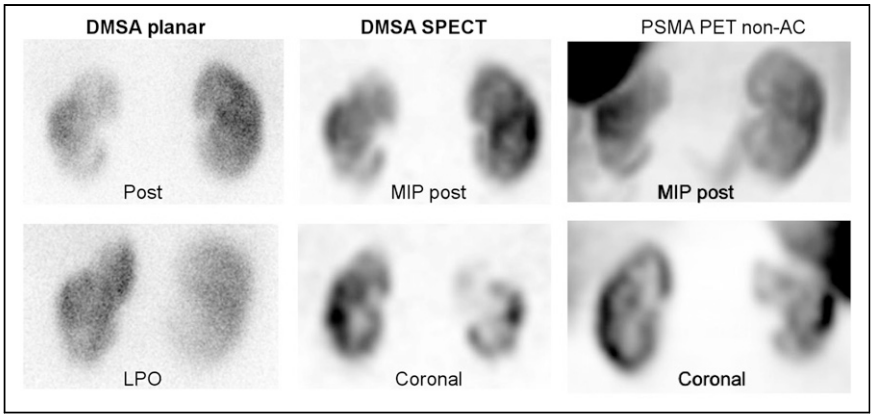

FIGURE 1. ^{99m}Tc-DMSA planar (posterior and left posterior oblique), ^{99m}Tc-DMSA SPECT (maximum-intensity projection in posterior view and selected coronal slice), and ^{68}Ga-PSMA-11 (non-AC maximum-intensity projection in posterior view and non-AC selected coronal slice) images demonstrating cortical defects or scars and reduced uptake in upper and lower poles of left kidney. Non-AC PET can be seen to have higher resolution than non-AC SPECT. LPO = left posterior oblique; MIP = maximum-intensity projection.

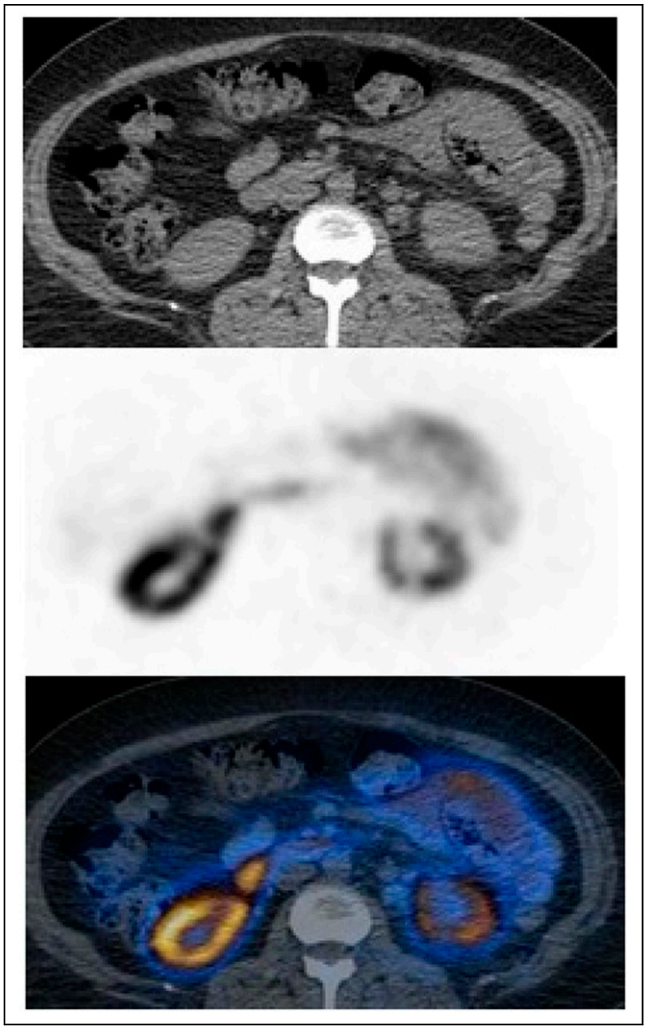

FIGURE 2. ^{68}Ga-PSMA-11 PET/CT (selected transaxial CT [top], PET [middle], and AC PET/CT [bottom]) images demonstrating reduced uptake in lower pole of left kidney and small cortical defect.

Potential new treatments may also prevent further scar development (*3*).

There is a shortage of DMSA cold kits in various countries, including the United States, and ^{99m}Tc-DMSA was therefore added to the drug-shortages list of the U.S. Food and Drug Administration in 2014 and has been commercially unavailable since then (*15*). Currently, there is not a good alternative to ^{99m}Tc-DMSA scanning. ^{99m}Tc-glucoheptonate is only partially concentrated in the kidneys and then is excreted in the urine (*1*). ^{68}Ga-alizarin red S was studied in animals and humans as a renal cortical PET radiotracer in the 1980s but was not used after that time (*16*). In a recent metaanalysis study, we compared ^{99m}Tc-DMSA scanning with MRI and found MRI and ^{99m}Tc-DMSA scanning to have overall equivalent sensitivity in detecting parenchymal changes in pyelonephritis, particularly in scar detection (*17*). MRI also has certain limitations and is not commonly in routine use to assess patients with pyelonephritis (*18*). We need new radiotracers, particularly PET tracers, that can selectively accumulate in the renal parenchyma and, compared with ^{99m}Tc-DMSA scanning, provide higher-resolution images of the kidneys, detect smaller cortical defects, and better quantify split renal function.

In our current patient, both ^{68}Ga-PSMA-11 PET (AC and non-AC) and ^{99m}Tc-DMSA scanning demonstrated cortical defects or scars in the left kidney with comparable image quality. Because of high splenic uptake from ^{68}Ga-colloid formation and some motion-related artifacts in the right kidney, image quality in our current patient was lower than in our previously reported patient (Fig. 3) (*14*). During the labeling procedure, formation of ^{68}Ga-colloid may occur and ^{68}Ga-colloid will accumulate in the spleen, liver, and bone marrow (*19*). Thin-layer chromatography is used to measure colloid content. We did not repeat the ^{68}Ga-PSMA-11 PET study in this patient because we did not want our patient to receive additional radiation exposure. Despite splenic uptake and some motion on the right side, AC and non-AC images successfully demonstrated scars in the left kidney.

Previously reported studies have demonstrated a good correlation between renal ^{99m}Tc-DMSA uptake and renal function tests such as effective renal plasma flow, glomerular filtration rate, and creatinine clearance (*20–24*). In our recently submitted retrospective study on 25 prostate cancer patients (Jan Henning Schierz et al., unpublished data, 2021), renal ^{68}Ga-PSMA-11 uptake appeared to correlate well with the results of renal function tests (creatinine and glomerular filtration rate).

There are certain advantages of ^{68}Ga-PSMA-11 PET over ^{99m}Tc-DMSA scanning, such as a shorter waiting time after injection (1 h vs. 3 h), a shorter half-life (68 min vs. 6 h),

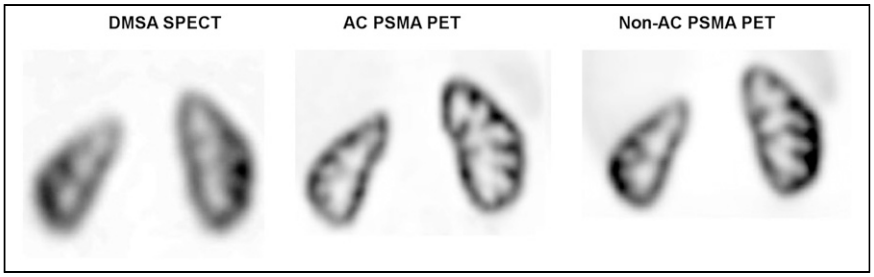

FIGURE 3. ^{99m}Tc-DMSA SPECT (selected coronal slice) and ^{68}Ga-PSMA-11 PET (AC and non-AC selected coronal slices) images of another patient with history of chronic recurrent pyelonephritis demonstrating mildly reduced uptake and cortical thinning in upper pole of right kidney with no parenchymal defects. Normal distribution of ^{68}Ga-PSMA-11 is seen, with only mild activity in liver and spleen.

and superior image quality, particularly with AC PET. The image acquisition time for our current patient was 20 min with ^{68}Ga-PSMA-11 PET because we used a low dose of activity to reduce the radiation dose to the patient (2 bed positions, 10 min per bed position, 48.1 MBq [1.3 mCi]). The image acquisition time for DMSA scanning was 55 min (30-min planar, 25-min SPECT). A longer acquisition time can cause patient discomfort and patient motion and result in image artifacts, requiring additional images and sedation in pediatric patients. The image acquisition time with ^{68}Ga-PSMA-11 PET can be further reduced to 6–7 min per bed position for 74 MBq (2 mCi), 4–5 min per bed position for 111 MBq (3 mCi), and 2–3 min per bed position for 148 MBq (4 mCi), but the kidney and effective doses will increase with higher activities. As we reported in our previous articles, absorbed adult kidney doses of ^{68}Ga-PSMA-11 and ^{99m}Tc-DMSA are 0.24 and 0.18 mGy/MBq, respectively, and effective adult doses are 0.022 and 0.0088 mSv/MBq, respectively (*25*,*26*). In our previously reported patient, estimated effective doses of 111 MBq (3 mCi) of ^{99m}Tc-DMSA and 74 MBq (2 mCi) of ^{68}Ga-PSMA-11 were 0.98 and 1.63 mSv, respectively. In our current patient, 48.1 MBq (1.3 mCi) of ^{68}Ga-PSMA-11 yielded an effective dose of 1.05 mSv, which is similar to the effective dose of ^{99m}Tc-DMSA. The additional radiation dose from CT in PET/CT is low because it is a low-dose CT scan and covers only the region of the kidneys. Non-AC PET also provides high-quality images of the renal parenchyma as seen in our current patient and in previous reports, and low-dose CT can therefore be omitted.

PET/CT cameras provide higher-resolution images than standard γ-cameras. In our patient, even low-dose non-AC PET provided images higher in quality than—or comparable in quality to—^{99m}Tc-DMSA SPECT. SPECT/CT provides higher-resolution images than SPECT, but we intentionally did not perform SPECT/CT on our patient to reduce the radiation dose in this research patient. Overall, PET/CT is known to provide higher-resolution images than SPECT/CT. On the other hand, SPECT systems with cadmium-zinc-telluride detectors have better resolution than conventional scanners with sodium iodide detectors (*27*).

The use and availability of ^{68}Ga-PSMA ligands for prostate cancer have been increasing. Recently, ^{68}Ga-PSMA-11 has been approved by the Food and Drug Administration for prostate cancer imaging. One limitation of ^{68}Ga-PSMA-11 PET is that it costs more than ^{99m}Tc-DMSA scanning: approximately $450 and $300, respectively, in our institute.

Quantification of uptake for each kidney showed results similar to those of ^{99m}Tc-DMSA scanning and ^{68}Ga-PSMA-11 PET. Because of high splenic uptake and limitations in our software, we could not perform automated volume-of-interest analysis on PSMA images, but in our recently submitted study, automated volume-of-interest analysis successfully provided total counts, volume, and SUVs for each kidney.

In our current patient, and in our previous patient with chronic pyelonephritis, ^{68}Ga-PSMA-11 PET appears to be a potential alternative to ^{99m}Tc-DMSA scanning. As discussed for our previous patient, its biodistribution and radiation dose in the pediatric population are not known, and further work is required to understand its mechanism of uptake, to determine the optimal injected activity, and to determine its dosimetry before its use as a renal cortical tracer can be supported.

CONCLUSION

The renal cortical scars caused by pyelonephritis were demonstrated well by ^{68}Ga-PSMA-11 PET.

DISCLOSURE

No potential conflict of interest relevant to this article was reported.

ACKNOWLEDGMENT

^{68}Ga-PSMA ligands are investigational PET radiotracers and as of now have not been approved by the U.S. Food and Drug Administration or European Medicines Agency. This article is about off-label use of ^{68}Ga-PSMA-11 for renal PET/CT imaging in adults.

REFERENCES

1. Mandell GA, Eggli DF, Gilday DL, et al. Procedure guideline for renal cortical scintigraphy in children. Society of Nuclear Medicine. *J Nucl Med.* 1997;38:1644–1646.
2. Sarikaya I, Sarikaya A. Current status of radionuclide renal cortical imaging in pyelonephritis. *J Nucl Med Technol.* 2019;47:309–312.
3. Murugapoopathy V, McCusker C, Gupta IR. The pathogenesis and management of renal scarring in children with vesicoureteric reflux and pyelonephritis. *Pediatr Nephrol.* 2020;35:349–357.
4. Afshar-Oromieh A, Avtzi E, Giesel FL, et al. The diagnostic value of PET/CT imaging with the ^{68}Ga-labelled PSMA ligand HBED-CC in the diagnosis of recurrent prostate cancer. *Eur J Nucl Med Mol Imaging.* 2015;42:197–209.

5. Sonni I, Eiber M, Fendler WP, et al. Impact of ^{68}Ga-PSMA-11 PET/CT on staging and management of prostate cancer patients in various clinical settings: a prospective single-center study. *J Nucl Med.* 2020;61:1153–1160.
6. Fendler WP, Eiber M, Beheshti M, et al. ^{68}Ga-PSMA PET/CT: joint EANM and SNMMI procedure guideline for prostate cancer imaging—version 1.0. *Eur J Nucl Med Mol Imaging.* 2017;44:1014–1024.
7. Silver DA, Pellicer I, Fair WR, Heston WD, Cordon-Cardo C. Prostate-specific membrane antigen expression in normal and malignant human tissues. *Clin Cancer Res.* 1997;3:81–85.
8. Mhawech-Fauceglia P, Zhang S, Terracciano L, et al. Prostate-specific membrane antigen (PSMA) protein expression in normal and neoplastic tissues and its sensitivity and specificity in prostate adenocarcinoma: an immunohistochemical study using multiple tumour tissue microarray technique. *Histopathology.* 2007;50:472–483.
9. Cunha AC, Weigle B, Kiessling A, Bachmann M, Rieber EP. Tissue-specificity of prostate specific antigens: comparative analysis of transcript levels in prostate and non-prostatic tissues. *Cancer Lett.* 2006;236:229–238.
10. Baccala A, Sercia L, Li J, Heston W, Zhou M. Expression of prostate-specific membrane antigen in tumor-associated neovasculature of renal neoplasms. *Urology.* 2007;70:385–390.
11. Ristau BT, O'Keefe DS, Bacich DJ. The prostate-specific membrane antigen: lessons and current clinical implications from 20 years of research. *Urol Oncol.* 2014; 32:272–279.
12. Sarikaya I, Elgazzar AH, Alfeeli MA, Sarikaya A. Can gallium-68 prostate-specific membrane antigen ligand be a potential radiotracer for renal cortical positron emission tomography imaging? *World J Nucl Med.* 2018;17:126–129.
13. Sarikaya I. ^{68}Ga-PSMA ligand as potential ^{99m}Tc-DMSA alternative. *J Nucl Med.* 2019;60(11):12N.
14. Sarikaya I, Alqallaf A, Sarikaya A. Renal cortical ^{68}Ga-PSMA-11 PET and ^{99m}Tc-DMSA images. *J Nucl Med Technol.* 2021;49:30–33.
15. Lim R, Bar-Sever Z, Treves ST. Is availability of ^{99m}Tc-DMSA insufficient to meet clinical needs in the United States? A survey. *J Nucl Med.* 2019;60(8):14N–16N.
16. Schuhmacher J, Maier-Borst W, Wellman HN. Liver and kidney imaging with Ga-68 labeled dihydroxyanthraquinones. *J Nucl Med.* 1980;21:983–987.
17. Sarikaya I, Albatineh AN, Sarikaya A. ^{99m}Tc-dimercaptosuccinic acid scan versus MRI in pyelonephritis: a meta-analysis. *Nucl Med Commun.* 2020; 41:1143–1152.
18. Mervak BM, Altun E, McGinty KA, et al. MRI in pregnancy: indications and practical considerations. *J Magn Reson Imaging.* 2019;49:621–631.
19. Brom M, Franssen GM, Joosten L, Gotthardt M, Boerman OC. The effect of purification of Ga-68-labeled exendin on in vivo distribution. *EJNMMI Res.* 2016; 6:65.
20. Taylor A Jr, Kipper M, Witztum K. Calculation of relative glomerular filtration rate and correlation with delayed technetium-99m DMSA imaging. *Clin Nucl Med.* 1986;11:28–31.
21. Taylor A. Quantitation of renal function with static imaging agents. *Semin Nucl Med.* 1982;12:330–344.
22. Kawamura J, Hosokawa S, Yoshida O, et al. Validity of ^{99m}Tc dimercaptosuccinic acid renal uptake for an assessment for individual kidney function. *J Urol.* 1978; 119:305–309.
23. Daly MJ, Jones W, Rudd TG, Tremann J. Differential renal function using technetium-99m dimercaptosuccinic acid (DMSA): in vitro correlation. *J Nucl Med.* 1979;20:63–66.
24. Groshar D, Embon OM, Frenkel A, Front D. Renal function and technetium-99m-dimercaptosuccinic acid uptake in single kidneys: the value of in vivo SPECT quantitation. *J Nucl Med.* 1991;32:766–768.
25. Mattsson S, Johansson L, Leide Svegborn S, et al. Radiation dose to patients from radiopharmaceuticals: a compendium of current information related to frequently used substances. *Ann ICRP.* 2015;44:7–321.
26. Sandgren K, Johansson L, Axelsson J, et al. Radiation dosimetry of [^{68}Ga]PSMA-11 in low-risk prostate cancer patients. *EJNMMI Phys.* 2019;6:2.
27. Daghighian F, Sumida R, Phelps ME. PET imaging: an overview and instrumentation. *J Nucl Med Technol.* 1990;18:5–13.